Biochemical and Biophysical Research Communications 439 (2013) 142–147

Contents lists available at ScienceDirect

Biochemical and Biophysical Research Communications

journal homepage: www.elsevier.com/locate/ybbrc

Senescence marker protein 30 inhibits angiotensin II-induced cardiac hypertrophy and diastolic dysfunction

Tomofumi Misaka [a], Satoshi Suzuki [a], Makiko Miyata [a], Atsushi Kobayashi [a], Akihito Ishigami [b], Tetsuro Shishido [c], Shu-ichi Saitoh [a], Isao Kubota [c], Yasuchika Takeishi [a,*]

[a] Department of Cardiology and Hematology, Fukushima Medical University, Fukushima, Japan
[b] Molecular Regulation of Aging, Tokyo Metropolitan Institute of Gerontology, Tokyo, Japan
[c] First Department of Internal Medicine, Yamagata University School of Medicine, Yamagata, Japan

ARTICLE INFO

Article history:
Received 30 July 2013
Available online 9 August 2013

Keywords:
Cardiac remodeling
Oxidative stress
Aging
Angiotensin II
Transgenic mouse

ABSTRACT

Background and objective: Senescence marker protein 30 (SMP30) is assumed to behave as an anti-aging factor. Recently, we have demonstrated that deficiency of SMP30 exacerbates angiotensin II-induced cardiac hypertrophy, dysfunction and remodeling, suggesting that SMP30 may have a protective role in the heart. Thus, this study aimed to test the hypothesis that up-regulation of SMP30 inhibits cardiac adverse remodeling in response to angiotensin II.
Methods: We generated transgenic mice with cardiac-specific overexpression of SMP30 gene using α-myosin heavy chain promoter. Transgenic mice and wild-type littermate mice were subjected to continuous angiotensin II infusion (800 ng/kg/min).
Results: After 14 days, heart weight and left ventricular weight were lower in transgenic mice than in wild-type mice, although blood pressure was similarly elevated during angiotensin II infusion. Cardiac hypertrophy and diastolic dysfunction in response to angiotensin II were prevented in transgenic mice compared with wild-type mice. The degree of cardiac fibrosis by angiotensin II was lower in transgenic mice than in wild-type mice. Angiotensin II-induced generation of superoxide and subsequent cellular senescence were attenuated in transgenic mouse hearts compared with wild-type mice.
Conclusions: Cardiac-specific overexpression of SMP30 inhibited angiotensin II-induced cardiac adverse remodeling. SMP30 has a cardio-protective role with anti-oxidative and anti-aging effects and could be a novel therapeutic target to prevent cardiac hypertrophy and remodeling due to hypertension.

1. Introduction

Senescence marker protein 30 (SMP30), a 34-kDa protein originally discovered in rat liver, is a marker of aging because its expression is decreased with age in an androgen-independent manner [1]. SMP30 gene is located in the p11.3–q11.2 segment of the X chromosome and highly conserved among vertebrates, indicating a crucial physiological function of SMP30 in mammals [2]. Moreover, SMP30 is widely distributed in almost all organs including the heart. Previous studies conducted using SMP30 knockout (KO) mice have reported that SMP30 has protective effects against age-associated oxidative stress in brain and lungs [3,4].

However, the functional role of SMP30 in the heart has not been fully elucidated. We have recently demonstrated using SMP30-KO mice that absence of SMP30 exacerbates angiotensin II-induced generation of reactive oxygen species, cardiac remodeling and dysfunction, suggesting that SMP30 has a protective role with anti-oxidative effects in the heart [5]. Here, we investigated whether up-regulation of cardiac SMP30 gene inhibits generation of reactive oxygen species, cardiac hypertrophy and remodeling in response to angiotensin II. We generated transgenic mice with cardiac-specific overexpression of SMP30 gene and tested the

Abbreviations: SMP30, senescence marker protein 30; IVS, intraventricular septal thickness; PW, posterior wall thickness; LVEDD, left ventricular end-diastolic dimension; LVESD, left ventricular end-systolic dimension; FS, left ventricular fractional shortening; E, peak early diastolic left ventricular filling velocity; A, peak atrial filling velocity; E′, early diastolic mitral annular velocity; A′, atrial mitral annular velocity; HW, heart weight; LVW, left ventricular weight; BW, body weight; TL, tibial length; DHE, dihydroethidium; SA-β-gal, senescence-associated β-galactosidase.

* Corresponding author. Address: Department of Cardiology and Hematology, Fukushima Medical University, 1 Hikarigaoka, Fukushima 960-1295, Japan. Fax: +81 24 548 1821.
E-mail address: takeishi@fmu.ac.jp (Y. Takeishi).

0006-291X
http://dx.doi.org/10.1016/j.bbrc.2013.08.002

hypothesis that SMP30 prevents angiotensin II-induced cardiac remodeling and dysfunction using a gain-of-functional approach in vivo.

2. Material and methods

2.1. Animals

The investigations conformed to the Guide for the Care and Use of Laboratory Animals published by the US National Institutes of Health (NIH publication, 8th Edition, 2011). Our research protocol was approved by the institutional review board, and all animal experiments were conducted in accordance with the guidelines of Fukushima Medical University Animal Research Committee.

Transgenic mice with cardiac-specific overexpression of SMP30 gene (SMP30-TG) were created using standard techniques with murine α-myosin heavy chain gene promoter (a kind gift from Dr. J. Robbins, Children's Hospital Research Foundation, Cincinnati, OH) as we previously reported [6,7]. The transgene composed of the α-myosin heavy chain gene promoter, murine SMP30 cDNA, and a poly A tail of the human growth hormone. We microinjected the DNA construct into the pronuclei of single cell fertilized mouse embryos to generate transgenic mice. To detect the exogenous SMP30 gene, genomic DNA was extracted from the tail tissues of 3–4-weeks-old pups, and polymerase chain reaction (PCR) was performed with one primer specific for the α-myosin heavy chain gene promoter and another primer specific for the SMP30 as reported previously [6,7].

2.2. Experimental protocol

Age-matched (12–16 weeks) male SMP30-TG mice and wild-type (WT) littermate mice were randomly divided into angiotensin II or control saline group. After anesthetizing the mice by intraperitoneal injection of pentobarbital (50 mg/kg body weight), an osmotic minipump (ALZET micro-osmotic pump MODEL 1002, DURECT Co., Cupertino, CA) was subcutaneously implanted, and angiotensin II (800 ng/kg per minute) or normal saline was continuously infused for 14 days [5,8].

2.3. Measurement of vitamin C

Total vitamin C levels in the heart were measured by the dinitrophenylhydrazine method according to the manufacturer's protocol (SHIMA Laboratories Co. Ltd., Tokyo, Japan) [9].

2.4. Measurements of blood pressure and heart rate

After subcutaneous infusion of angiotensin II or saline, the systolic, mean and diastolic blood pressures and heart rate were measured by the tail-cuff method using a programmable sphygmomanometer (BP-98A-L, Softron, Tokyo, Japan) under free from anesthesia [5,8].

2.5. Echocardiography

After 2 weeks of angiotensin II infusion, echocardiography was performed using Vevo 2100 High-Resolution In Vivo Imaging System (Visual Sonics Inc., Toronto, Canada) with a high-resolution 40-MHz imaging transducer as previous reports described [5,7]. Mice were lightly anesthetized by titrating isoflurane (0.5–1.5%) to achieve a heart rate of around 400 beats/min. Parasternal long-axis, short-axis, and apical four-chamber two-dimensional images were acquired. With the use of the M-mode image from the parasternal short-axis view at the papillary muscle level, intraventricular septal thickness (IVS), posterior wall thickness (PW), left ventricular end-diastolic dimension (LVEDD), and left ventricular end-systolic dimension (LVESD) were measured [5–7]. The percentage of left ventricular fractional shortening (FS) was calculated as $100 \times ((\mathrm{LVEDD}-\mathrm{LVESD})/\mathrm{LVEDD})$. Left ventricular mass was calculated as $1.053 \times ((\mathrm{LVEDD}+\mathrm{LVESD}+\mathrm{IVS})^3-\mathrm{LVEDD}^3)$. Pulse Doppler images were taken with the apical four-chamber view to record the mitral Doppler inflow spectrum [5,10,11]. Peak early diastolic left ventricular filling velocity (E) and peak atrial filling velocity (A) were measured. Pulse wave tissue Doppler imaging was taken at the septal side of mitral annulus. Early diastolic mitral annular velocity (E') and atrial mitral annular velocity (A') were measured. The ratio of E to A (E/A) and the ratio of E to E' (E/E') were calculated [5,10,11]. All measurements were obtained from 3 cardiac cycles and the data were averaged.

2.6. Histopathological analysis

After continuous infusion of angiotensin II or saline for 14 days, mice were sacrificed by cervical dislocation and hearts were rapidly excised. Whole heart weight (HW) and left ventricular weight (LVW) were measured and normalized by body weight (BW) and tibial length (TL). The paraffin-embedded heart sections were stained with hematoxylin-eosin or Elastica-Masson. The photomicrographs of the sections stained with hematoxylin-eosin were digitally taken, and cross-sectional area of cardiomyocytes was measured using NIH ImageJ software (National Institutes of Health, Bethesda, Maryland) [5,6]. Myocardial interstitial fibrosis was assessed by Elastica-Masson staining. The area of fibrosis, which was stained with blue collagen, was determined using Adobe Photoshop CS2 (Adobe, San Jose, CA), and fibrosis fraction was calculated as the ratio of the blue color area to total cardiac area [5–7].

2.7. Assessment of superoxide generation

The excised heart tissue was immediately frozen in liquid nitrogen with optimal cutting temperature compound and sectioned at 10-μm thickness [5]. The section was incubated with 10 μmol/l dihydroethidium (DHE, Sigma–Aldrich Co., St. Louis, MO) at 37 °C for 30 min. The fluorescent images were acquired using fluorescence microscope (Olympus IX71, OLYMPUS Optical Co., Tokyo, Japan) and the mean DHE fluorescence intensity of cardiomyocytes, which were in 20 randomly selected fields in each section, was quantitated with NIH imageJ software [5,12].

2.8. Senescence-associated β-galactosidase activity

Senescence-associated β-galactosidase (SA-β-gal) staining was performed using fresh frozen sections (4-μm thickness) of the left ventricular tissues according to the manufacturer's protocol (Bio-Vision Inc., Mountain View, CA) [5,13]. SA-β-gal positive cells were visualized as blue color under light microscopy, and positive cells for SA-β-gal activity were counted in 10 sections of each sample.

2.9. Reverse transcription polymerase chain reaction

Total RNA was extracted from the snap-frozen left ventricle using TRIzol reagent (Invitrogen, Carlsbad, CA). The RNAs were reverse-transcribed (RT) into first strand cDNAs, and the cDNAs were subjected to PCR with PrimeScript RT-PCR Kit (Takara Bio Inc., Otsu, Japan) according to the manufacturer's instructions [5–7]. Primers were designed on the basis of GenBank sequences (p21, NM_001111099 and β-actin, NM_007393). Amplified PCR products were resolved on 1% agarose gels and visualized by ethidium bromide staining under ultraviolet illumination and photographed.

The optical density of the bands was quantified using NIH imageJ software. Gene expression was normalized by β-actin as the internal standard and the results were expressed as a fold increase over WT control [5–7].

2.10. Statistical analysis

All data were expressed as mean ± standard deviation (SD). Comparisons of vitamin C levels at basal conditions between WT mice and SMP30-TG mice were performed by an unpaired *t*-test. All other parameters were evaluated by two-way analysis of variance (ANOVA) followed by multiple comparisons with Bonferroni test using SPSS Statistics 17.0 (SPSS Japan Inc., Tokyo, Japan). A probability value <0.05 was considered statistically significant.

3. Results

3.1. Generation of SMP30-TG mice

Gene and protein expression levels of SMP30 were augmented about ten-fold and five-fold in SMP30-TG mouse hearts compared with WT mice, respectively. No neonatal and adult deaths were seen in SMP30-TG mice. There was no abnormal finding on echocardiography and microscopic examinations of multiple histological sections of the heart (data not shown) in SMP30-TG mice. Cardiac tissue concentration of vitamin C levels was not different between SMP30-TG mice and WT mice (46.5 ± 6.6 vs. 45.7 ± 7.0 μg/g tissue).

3.2. Overexpression of SMP30 blocked angiotensin II-induced cardiac hypertrophy and fibrosis

BW, HW and LVW were similar between control WT mice and SMP30-TG mice (Table 1). After angiotensin II infusion for 14 days, both systolic and diastolic blood pressures were similarly elevated in WT mice and SMP30-TG mice (Table 1). However, HW, LVW, HW/BW, LVW/BW, HW/TL, and LVW/TL were significantly lower in SMP30-TG mice than in WT mice after angiotensin II infusion. The cardiomyocyte cross sectional area was not different between control WT and SMP30 TG mice (Fig. 1). Although angiotensin II infusion increased cardiomyocyte cross sectional area, the increase was less in SMP30-TG mice than in WT mice as shown in Fig. 1.

Table 1
Gravimetric and hemodynamic data of WT and SMP30-TG mice.

	Control		Angiotensin II	
	WT	SMP30-TG	WT	SMP30-TG
Gravimetric data				
BW, g	26.8 ± 1.8	27.5 ± 1.8	25.8 ± 1.4	26.3 ± 1.8
HW, mg	129 ± 13	134 ± 8	163 ± 8**	145 ± 11**††
LVW, mg	90 ± 11	93 ± 9	123 ± 8**	110 ± 10**†
HW/BW, mg/g	4.8 ± 0.4	4.9 ± 0.3	6.3 ± 0.5**	5.6 ± 0.7**†
LVW/BW, mg/g	3.3 ± 0.3	3.4 ± 0.2	4.8 ± 0.4**†	4.2 ± 0.6**†
HW/TL, mg/mm	6.1 ± 0.6	6.3 ± 0.3	7.7 ± 0.4**	6.8 ± 0.5**†
LVW/TL, mg/mm	4.2 ± 0.5	4.4 ± 0.4	5.8 ± 0.4**	5.2 ± 0.4**†
Hemodynamic data				
HR, bpm	595 ± 84	576 ± 63	513 ± 80	524 ± 59
SBP, mmHg	104 ± 5	105 ± 8	146 ± 8**	146 ± 6**
DBP, mmHg	68 ± 9	64 ± 6	93 ± 13**	96 ± 11**
MAP, mmHg	80 ± 8	78 ± 6	111 ± 11**	113 ± 9**

BW, indicates body weight; HW, heart weight; LVW, left ventricular weight; TL, tibial length; HR, heart rate; SBP, systolic blood pressure; DBP, diastolic blood pressure; and MAP, mean arterial pressure. Data are presented as mean ± SD from 10 to 15 mice in each group.
**$P < 0.01$ vs. control in the same strain mice.
†$P < 0.05$.
††$P < 0.01$ vs. angiotensin II-infused WT mice.

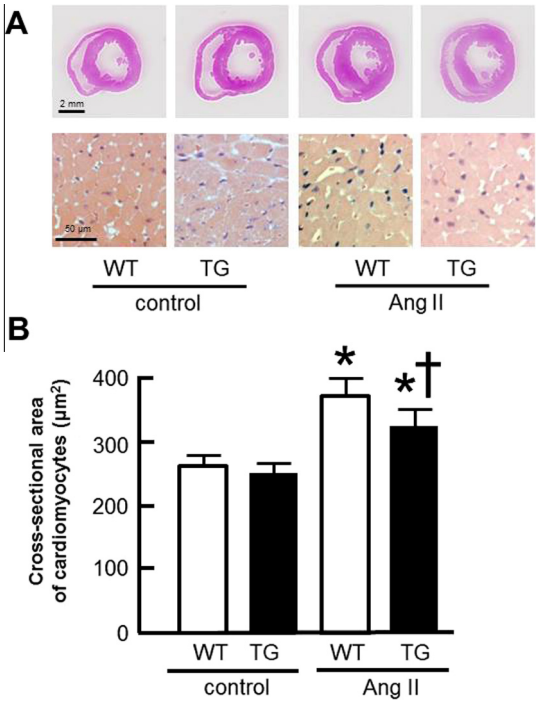

Fig. 1. Cardiac hypertrophy in WT mice and SMP30-TG mice after angiotensin II infusion. (A) Top, Representative images of light micrographs of hearts from WT and SMP30-TG mice with and without angiotensin II infusion. Bottom, hematoxylin and eosin staining of myocardial cross sections. (B) Quantitative analysis of cross-sectional area of cardiomyocytes from the left ventricle. Data are presented as mean ± SD from 6 to 8 mice in each group. *$P < 0.01$ vs. control in the same strain mice; †$P < 0.01$ vs. angiotensin II- infused WT mice.

There were no significant differences in fibrosis fraction at basal condition between WT and SMP30-TG mice (Fig. 2). Although angiotensin II induced interstitial fibrosis in both WT and SMP30 TG mice, the extent of myocardial fibrosis was significantly lower in SMP30-TG mice than in WT mice after angiotensin II stimulation as shown in Fig. 2. These data revealed that the cardiac-specific

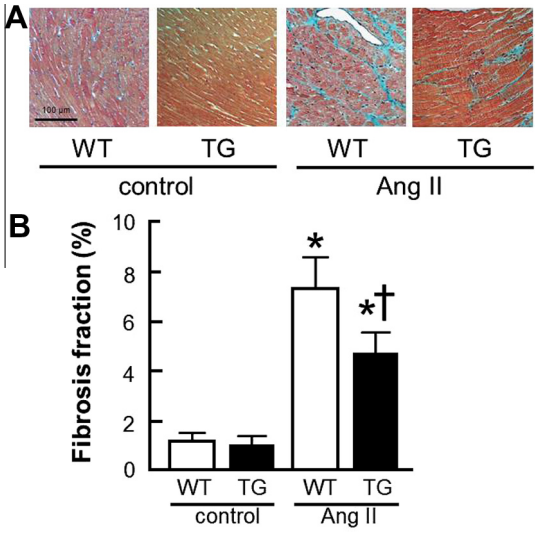

Fig. 2. Myocardial fibrosis in WT mice and SMP30-TG mice after angiotensin II infusion. (A) Representative images of Elastica-Masson staining of myocardial sections. (B) The percent area of myocardial interstitial fibrosis in the left ventricle. Data are presented as mean ± SD from 6 to 8 mice in each group. *$P < 0.01$ vs. control in the same strain mice; †$P < 0.01$ vs. angiotensin II-infused WT mice.

overexpression of SMP30 improved angiotensin II-induced cardiac hypertrophy and fibrosis, independently of elevated blood pressure.

3.3. SMP30 preserved angiotensin II-induced cardiac diastolic function

Echocardiography showed that each parameter was not different between control WT mice and SMP30-TG mice (Table 2). After angiotensin II infusion, thickness of intraventricular septum and posterior wall, and calculated LV mass in SMP30-TG mice were significantly lower than those in WT mice. Left ventricular ejection fraction did not change in either WT mice or SMP30-TG mice following angiotensin II infusion. To evaluate left ventricular diastolic function, pulse Doppler imaging of left ventricular inflow and pulse wave tissue Doppler imaging at the mitral annulus were performed. In SMP30-TG mice, 40% of mice (4/10) showed a relaxation abnormality pattern (E/A < 1), whereas all of WT mice (10/10) showed a pseudo-normalization pattern (E/A > 1) after angiotensin II infusion. In addition, E/E' in SMP30-TG mice was lower than that in WT mice after angiotensin II stimulation as shown in Table 2. These data indicated that not only cardiac hypertrophy but also diastolic function was preserved in SMP30-TG mice after angiotensin II stimulation.

3.4. SMP30 blocked angiotensin II-induced myocardial oxidative stress

To assess the effect of SMP30 expression on myocardial oxidative stress, we performed DHE staining, which indicates the superoxide levels. Left ventricular sections with the fluorescence probe DHE demonstrated that superoxide generation was not different between WT mice and SMP30-TG mice at basal condition (Fig. 3). However, after angiotensin II stimulation, the increase of superoxide generation in SMP30-TG mice was significantly lower than that in WT mice as shown in Fig. 3. This finding demonstrated that cardiac-specific overexpression of SMP30 attenuated angiotensin II-induced superoxide generation.

Table 2
Echocardiography of WT and SMP30-TG mice.

	Control		Angiotensin II	
	WT	SMP30-TG	WT	SMP30-TG
IVS, mm	0.71 ± 0.05	0.73 ± 0.06	0.91 ± 0.07**	0.84 ± 0.11**,††
PW, mm	0.78 ± 0.07	0.75 ± 0.04	0.95 ± 0.10**	0.88 ± 0.07**,†
LVEDD, mm	3.77 ± 0.37	3.70 ± 0.26	3.68 ± 0.31	3.53 ± 0.26
LVESD, mm	2.52 ± 0.32	2.54 ± 0.36	2.52 ± 0.35	2.44 ± 0.32
FS, %	33.2 ± 4.4	32.3 ± 6.1	31.8 ± 4.7	32.0 ± 5.3
EF, %	62.4 ± 6.7	60.9 ± 8.1	60.4 ± 7.1	60.7 ± 7.6
LV mass, mg	96.1 ± 18.2	90.7 ± 13.4	126.0 ± 16.5**	106.5 ± 9.4**,††
E velocity, mm/s	503 ± 63	513 ± 85	499 ± 95	442 ± 150
A velocity, mm/s	302 ± 93	312 ± 51	307 ± 110	292 ± 124
E/A	1.82 ± 0.70	1.67 ± 0.26	1.49 ± 0.23	1.09 ± 0.47
E' velocity, mm/s	18.7 ± 5. 5	18.3 ± 2.8	12.7 ± 3.7*	13.7 ± 3.3*
E/E'	29.0 ± 6.8	28.2 ± 3.6	42.2 ± 8.3**	32.6 ± 10.0**,†

IVS, indicates intraventricular septum; PW, posterior wall thickness; LVEDD, left ventricular end-diastolic dimension; LVESD, left ventricular end-systolic dimension; FS, fractional shortening; EF, ejection fraction; E, peak early diastolic left ventricular filling velocity; A, peak atrial filling velocity; and E', early diastolic mitral annular velocity.
Results are mean ± SD from 8 to 12 mice in each group.
* $P < 0.05$.
** $P < 0.01$ vs. control in same strain mice.
† $P < 0.05$.
†† $P < 0.01$ vs. angiotensin II-infused WT mice.

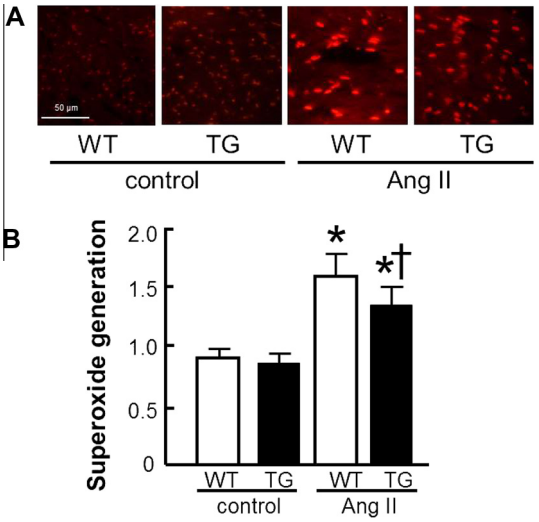

Fig. 3. Myocardial oxidative stress in WT mice and SMP30-TG mice after angiotensin II infusion. (A) Representative images of dihydroethidium (DHE) staining of frozen left ventricular tissues. (B) Bar graphs show quantification of superoxide generation. Results are mean ± SD from 5 to 6 mice in each group. *$P < 0.01$ vs. control in the same strain mice; †$P < 0.01$ vs. angiotensin II-infused WT mice.

3.5. SMP30 attenuated cellular senescence after angiotensin II infusion

Senescent cells can be identified by the expression of enzymatic SA-β-gal activity in left ventricular tissues. There were no SA β-gal positive cells in control WT mice and SMP30-TG mice (Fig. 4A). Angiotensin II induced SA-β-gal positive cells in left ventricular myocardium, and the numbers of SA-β-gal positive cells were significantly lower in SMP30-TG mice than in WT mice (Fig. 4A). To evaluate the gene expression of cell cycle inhibitor to confirm cardiac cellular senescence, we performed RT-PCR analysis. The results of RT-PCR demonstrated that p21 gene expression was significantly suppressed in SMP30-TG mice compared with WT mice after angiotensin II infusion (Fig. 4B). Neither p16 nor p53 gene expression was different between 2 groups (data not shown). These results indicated that overexpression of SMP30 effectively attenuated cardiac cellular senescence after angiotensin II infusion by p21-dependent pathway.

4. Discussion

In this study, we demonstrated that cardiac-specific overexpression of SMP30 inhibited angiotensin II-induced cardiac hypertrophy, fibrosis and diastolic dysfunction. SMP30 also suppressed superoxide generation and senescence markers including p21 gene expression after angiotensin II infusion. Recently, we have shown that deficiency of SMP30 exacerbates angiotensin II-induced cardiac hypertrophy, left ventricular dysfunction and adverse remodeling. Interestingly, the present data of SMP30-TG mice reversed those phenotypes observed in SMP30-KO mice. These data suggest that SMP30 could be a novel therapeutic target to prevent cardiac remodeling and diastolic dysfunction, especially due to hypertension.

SMP30 gene is highly conserved among vertebrates, indicating a crucial physiological function of SMP30 in all mammals [2]. Moreover, SMP30 is widely distributed in almost all organs including heart. Calorie restriction, which is thought to be anti-aging and anti-oxidative actions, effectively suppressed age-related down-regulation of SMP30 expression [14]. These findings suggested that SMP30 expression is influenced by oxidative stress, and SMP30 is assumed to behave as an anti-aging factor. While the physiological function of SMP30 remains entirely unclear, previous studies have

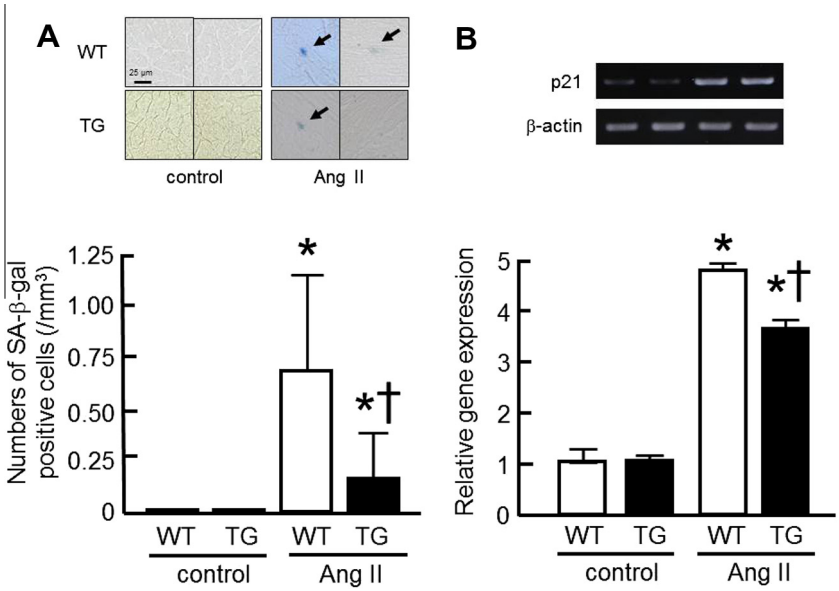

Fig. 4. Senescence markers in the hearts of WT mice and SMP30-TG mice after angiotensin II infusion. (A) Senescent cells were detected by SA β-gal staining of left ventricular tissue sections (upper panels), and the numbers of SA β-gal-positive cells were counted (lower bar graph). (B) The mRNA expression levels of p21 gene were analyzed by RT-PCR. Expression levels of p21 gene were normalized by β-actin. Results are mean ± SD from 6 to 8 mice in each group. $^{*}P < 0.01$ vs. control in the same strain mice; $^{\dagger}P < 0.01$ vs. angiotensin II-infused WT mice.

shown that SMP30 prevents oxidative stress and the lack of SMP30 causes various dysfunctions of organs during aging process [3,4]. In addition, it has been reported that SMP30 has multiple functions such as Ca^{2+} regulator (named as regucalcin) [15], anti-oxidant [16], and enzymatic ability to hydrolyze diisopropyl phosphorofluoridate [17]. Recently, SMP30 has been identified as glucolactonase, which is a key enzyme for L-ascorbic acid (vitamin C) biosynthesis in mammals, although human beings are unable to synthesize vitamin C because of mutations in L-gulonolactone oxidase [18]. In the present study, tissue concentrations of vitamin C level were not different between WT mice and SMP30-TG mice.

Aging is an important risk factor of cardiovascular diseases such as hypertension, left ventricular hypertrophy and heart failure [19]. With aging, the heart shows age-related changes in cardiac structure and function [20]. An increase in oxidant stress with aging is implicated in age-related cardiac remodeling [21]. On the other hand, it is appreciated that renin-angiotensin system (RAS) plays a key role in the development of cardiac remodeling and heart failure. Many experimental studies have showed that RAS activation mediates oxidative stress in the heart, and therefore, inhibition of RAS may reverse age-related cardiac remodeling by suppressive effects of cardiac oxidative stress [22]. Thus, it is considered that control of oxidative stress may have influence on cardiac remodeling and that suppression of oxidative stress can protect the heart against aging. In the present study, angiotensin II-induced superoxide generation was inhibited in the heart of SMP30-TG mice. In addition, cardiac cellular senescence due to angiotensin II was blocked in SMP30-TG mice.

In summary, cardiac-specific overexpression of SMP30 inhibited angiotensin II-induced cardiac hypertrophy, fibrosis and impaired diastolic function, suggesting that SMP30 has a cardio-protective role with anti-oxidative and anti-aging effects. Up-regulation of SMP30 could attenuate the development of heart failure and be a novel strategy to approach senescent cardiac diseases.

Acknowledgments

We thank Ms. Emiko Kaneda for the excellent technical assistance. This study was supported in part by a grant-in-aid for Scientific Research (No. 24591100) from the Japan Society for the Promotion of Science and the grants-in-aid from the Japanese Ministry of Health, Labor, and Welfare, Tokyo, Japan.

References

[1] T. Fujita, K. Uchida, N. Maruyama, Purification of senescence marker protein-30 (SMP30) and its androgen-independent decrease with age in the rat liver, Biochim. Biophys. Acta 1116 (1992) 122–128.
[2] T. Fujita, J.L. Mandel, T. Shirasawa, et al., Isolation of cdna clone encoding human homologue of senescence marker protein-30 (SMP30) and its location on the X chromosome, Biochim. Biophys. Acta 1263 (1995) 249–252.
[3] T.G. Son, Y. Zou, K.J. Jung, et al., SMP30 deficiency causes increased oxidative stress in brain, Mech. Ageing Dev. 127 (2006) 451–457.
[4] T. Sato, K. Seyama, Y. Sato, et al., Senescence marker protein-30 protects mice lungs from oxidative stress, aging, and smoking, Am. J. Respir. Crit. Care Med. 174 (2006) 530–537.
[5] T. Misaka, S. Suzuki, M. Miyata, et al., Deficiency of senescence marker protein 30 exacerbates angiotensin II-induced cardiac remodeling, Cardiovasc. Res. (2013) May 30 [Epub ahead of print].
[6] T. Arimoto, Y. Takeishi, H. Takahashi, et al., Cardiac-specific overexpression of diacylglycerol kinase zeta prevents Gq protein-coupled receptor agonist-induced cardiac hypertrophy in transgenic mice, Circulation 113 (2006) 60–66.
[7] T. Kitahara, Y. Takeishi, M. Harada, et al., High-mobility group box 1 restores cardiac function after myocardial infarction in transgenic mice, Cardiovasc. Res. 80 (2008) 40–46.
[8] A. Kobayashi, K. Ishikawa, H. Matsumoto, et al., Synergetic antioxidant and vasodilatory action of carbon monoxide in angiotensin II-induced cardiac hypertrophy, Hypertension 50 (2007) 1040–1048.
[9] C.S. Tsao, P.Y. Leung, M. Young, Effect of dietary ascorbic acid intake on tissue vitamin C in mice, J. Nutr. 117 (1987) 291–297.
[10] J. Du, J. Liu, H.Z. Feng, et al., Impaired relaxation is the main manifestation in transgenic mice expressing a restrictive cardiomyopathy mutation, R193H, in cardiac TnI, Am. J. Physiol. Heart Circ. Physiol. 294 (2008) H2604–2613.
[11] R.M. Wilson, D.S. De Silva, K. Sato, et al., Effects of fixed-dose isosorbide dinitrate/hydralazine on diastolic function and exercise capacity in hypertension-induced diastolic heart failure, Hypertension 54 (2009) 583–590.
[12] H. Machii, S. Saitoh, T. Kaneshiro, et al., Aging impairs myocardium-induced dilation in coronary arterioles: role of hydrogen peroxide and angiotensin, Mech. Ageing Dev. 131 (2010) 710–717.
[13] G.P. Dimri, X. Lee, G. Basile, et al., A biomarker that identifies senescent human cells in culture and in aging skin in vivo, Proc. Natl. Acad. Sci. U.S.A. 92 (1995) 9363–9367.
[14] K.J. Jung, A. Ishigami, N. Maruyama, et al., Modulation of gene expression of SMP-30 by LPS and calorie restriction during aging process, Exp. Gerontol. 39 (2004) 1169–1177.

[15] N. Shimokawa, M. Yamaguchi, Molecular cloning and sequencing of the cDNA coding for a calcium-binding protein regucalcin from rat liver, FEBS Lett. 327 (1993) 251–255.
[16] T.G. Son, S.J. Kim, K. Kim, et al., Cytoprotective roles of senescence marker protein 30 against intracellular calcium elevation and oxidative stress, Arch. Pharm. Res. 31 (2008) 872–877.
[17] J.S. Little, C.A. Broomfield, M.K. Fox-Talbot, et al., Partial characterization of an enzyme that hydrolyzes sarin, soman, tabun, and diisopropyl phosphorofluoridate (DFP), Biochem. Pharmacol. 38 (1989) 23–29.
[18] Y. Kondo, Y. Inai, Y. Sato, et al., Senescence marker protein 30 functions as gluconolactonase in L-ascorbic acid biosynthesis, and its knockout mice are prone to scurvy, Proc. Natl. Acad. Sci. U.S.A. 103 (2006) 5723–5728.
[19] E.G. Lakatta, D. Levy, Arterial and cardiac aging: major shareholders in cardiovascular disease enterprises. Part II: the aging heart in health: links to heart disease, Circulation 107 (2003) 346–354.
[20] E.G. Lakatta, Arterial and cardiac aging: major shareholders in cardiovascular disease enterprises. Part III: cellular and molecular clues to heart and arterial aging, Circulation 107 (2003) 490–497.
[21] M. Wang, J. Zhang, S.J. Walker, et al., Involvement of NADPH oxidase in age-associated cardiac remodeling, J. Mol. Cell. Cardiol. 48 (2010) 765–772.
[22] N. Ito, M. Ohishi, K. Yamamoto, et al., Renin-angiotensin inhibition reverses advanced cardiac remodeling in aging spontaneously hypertensive rats, Am. J. Hypertens. 20 (2007) 792–799.